Pergamon

International Journal of Machine Tools & Manufacture 43 (2003) 523–532

INTERNATIONAL JOURNAL OF
MACHINE TOOLS
& MANUFACTURE
DESIGN, RESEARCH AND APPLICATION

Fixed abrasive diamond wire machining—part I: process monitoring and wire tension force

W.I. Clark [a], A.J. Shih [b,*], C.W. Hardin [a], R.L. Lemaster [c], S.B. McSpadden [d]

[a] *Department of Mechanical and Aerospace Engineering, North Carolina State University, Raleigh, NC 27695, USA*
[b] *Department of Mechanical Engineering, University of Michigan, Ann Arbor, MI 48109, USA*
[c] *Department of Wood and Paper Science, North Carolina State University, Raleigh, NC 27695, USA*
[d] *High Temperature Materials Laboratory, Oak Ridge National Laboratory, Oak Ridge, TN 37831, USA*

Received 19 August 2002; received in revised form 17 September 2002; accepted 1 October 2002

Abstract

The process monitoring and mechanics of fixed abrasive diamond wire saw machining are investigated in this study. New techniques to affix diamond particles to a steel wire core have advanced to make this process feasible for the machining of ceramics, wood, and foam materials. Developments in fixed abrasive diamond wire machining are first reviewed. Advantages of using fixed abrasive diamond wire machining are then introduced. The process monitoring and signal processing techniques for measuring the cutting forces, wire speed, down feed rate, and wire bow angle in diamond wire saw machining are developed. The application of a capacitance sensor to measure the wire bow and a procedure to convert the wire bow to vertical cutting force in a rocking motion wire saw machine are developed. The tension force of the wire during cutting is also derived and discussed.

Keywords: Diamond wire saw; Wire saw machining; Process monitoring

1. Introduction

Slicing single crystal silicon into thin wafers with minimum warp, uniform thickness, and low kerf loss has revitalized the interest in wire saw machining technology, a concept that originated from the carpenter wire saw for wood machining. The early wire saw wafer slicing development in the 1990s applied a loose abrasive slurry on bare wire. During machining, a small portion of the abrasive is impregnated as third-body between the wire and workpiece to generate the cutting action. This process has been successfully implemented in silicon and silicon carbide wafer production using silicon carbide and diamond, respectively, as the loose abrasive.

To further reduce the processing time and to machine other harder and more difficult-to-machine ceramic materials, new diamond impregnated wires and wire saw machines that use the wire with fixed diamond abrasive have been developed. The goal of this research is to study the fixed abrasive diamond wire saw machining technologies, including process monitoring and signal processing, tension of the wire during cutting, and applications in wood and foam ceramics cutting.

Compared to traditional cutting methods, the fixed abrasive diamond wire has several advantages. First, the diamond wire saw could machine non-electrically conductive materials that cannot be cut by the electrical discharge machining (EDM). Second, the diamond wire can be looped or ganged around rollers to cut multiple thin wafers simultaneously. Third, the kerf loss for diamond wire saw machining is small. This is particularly attractive for machining high cost semi-conductor and wood materials. For example, the inner diamond saw blade for cutting semiconductor wafer has a kerf of about 0.30 and 0.38 mm for 150 and 200 mm diameter wafer, respectively. The loose and fixed abrasive wire saw can achieve less than 0.3 mm kerf for slicing larger, 300 mm diameter wafers. As shown in Fig. 1, this level of kerf loss, compared to that of high-end super thin saw blades for wood machining, is about an order of magnitude smaller. Another advantage of the fixed abrasive diamond is the

* Corresponding author. Tel.: +1-734-647-1766; fax: +1-734-936-0363.
E-mail address: shiha@umich.edu (A.J. Shih).

0890-6955/03/$ - see front matter © 2003 Published by Elsevier Science Ltd.
doi:10.1016/S0890-6955(02)00215-8

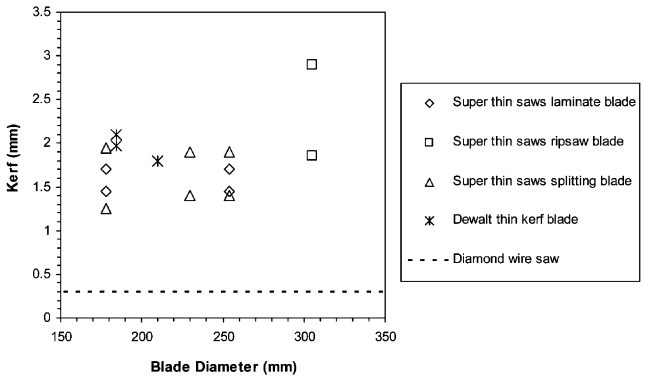

Fig. 1. Comparison of the kerf for super thin saw blades and diamond wire saw for wood machining.

freedom to change wire cutting directions and orientations, similar to that of wire EDM. With the assistance of in-process wire bow sensors, precision contour cutting using a fixed abrasive diamond wire saw is possible. Compared to circular saws and band saws, which cannot easily change cutting directions, the diamond wire saw is more flexible for cutting parts with complicated geometry. An example of a cedar slat cut by a diamond wire saw is shown in Fig. 2.

A review of the recent development of wire saw machining technologies is first presented. The process monitoring and signal processing techniques, including the measurement of cutting forces, wire bow, yoke down feed rate, and wire speed, and the mechanics of wire saw cutting are then presented.

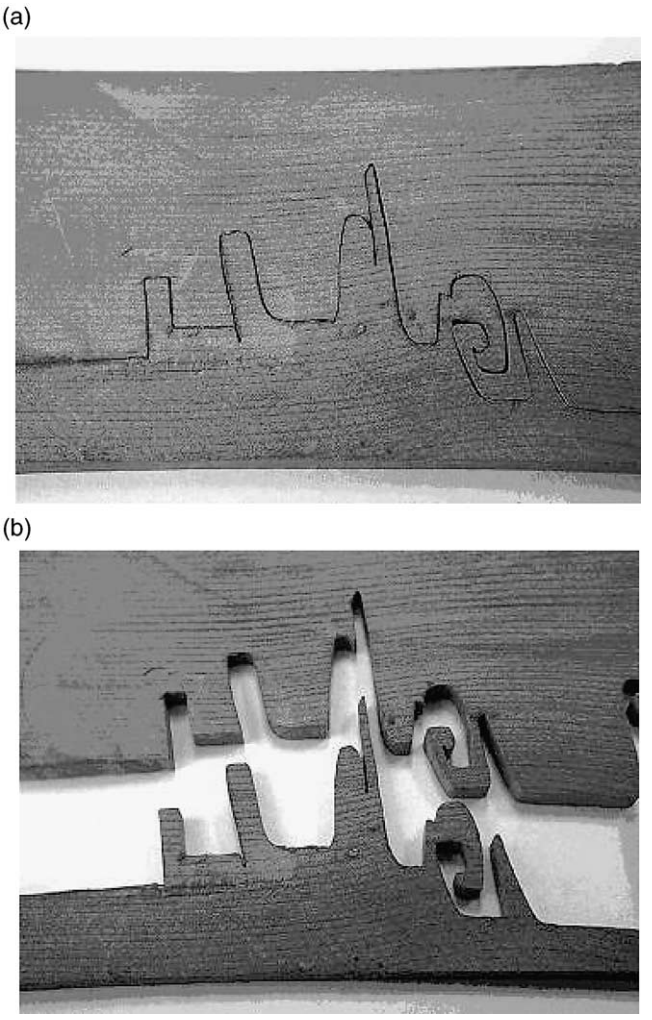

Fig. 2. A cedar slat machined by the diamond wire saw. (a) Trace of wire cut path; (b) Separation of two pieces after cutting.

2. Review of the development of wire saw technologies

In the past decade, several major technical developments in fixed abrasive diamond wire saw machining have emerged. Four new technologies are summarized as follows.

2.1. New metal bond diamond wire

New methods to firmly affix diamond to a thin, flexible wire have been developed. Fig. 3 shows examples of metal bond diamond wire from three different suppliers. The diamond wire from Supplier 1, as shown in Fig. 3(a), has the electroplated method bond, which is also treated by laser to improve diamond retention. An extra layer of metal bond is electroplated over the diamond, as shown in the close-up view of the diamond grit in Fig. 4(a), to further improve the bonding strength of the diamond and wire. Supplier 2 mechanically rolls the diamond grits into a steel wire. As shown in Fig. 3(b) and 4(b), diamond grits are exposed outside the wire to provide a good cutting action. Supplier 3 also uses the electroplating method to affix diamond to the wire. As shown in Fig. 3(c) and Fig. 4(c), smaller grit size diamond, which can reduce the damage on the cut surface, are used by Supplier 3. The trend in the past decade shows that diamond wire technologies are continuously evolving. The development of newer, more durable fixed abrasive diamond wires has broadened applications of diamond wire cutting.

2.2. High speed wire saw machine

Similar to high speed grinding, high wire speeds can reduce the cutting force on each diamond grit, lower the wire wear and diamond pull-out, and achieve higher material removal rates. The maximum wire speed on newly developed diamond wire saw machines is over 15 m/s.

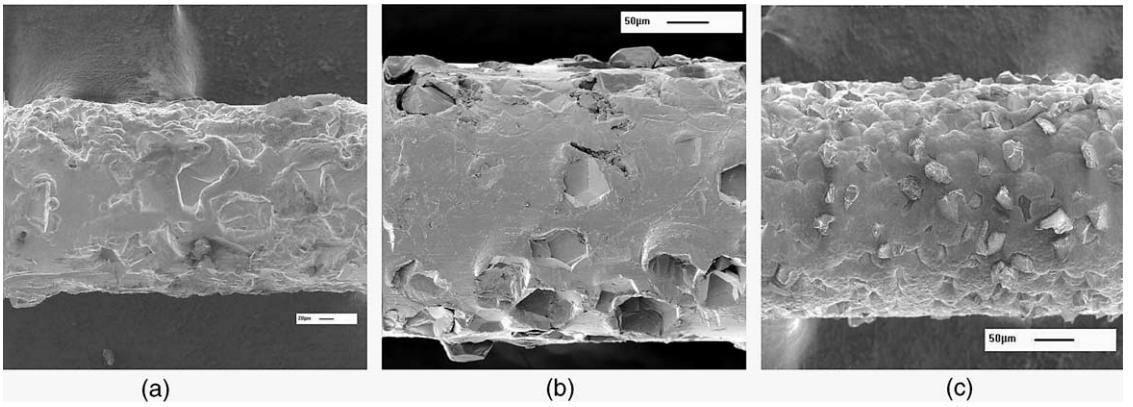

Fig. 3. SEM micrograph of the new diamond wires. (a) Supplier 1; (b) Supplier 2; (c) Supplier 3.

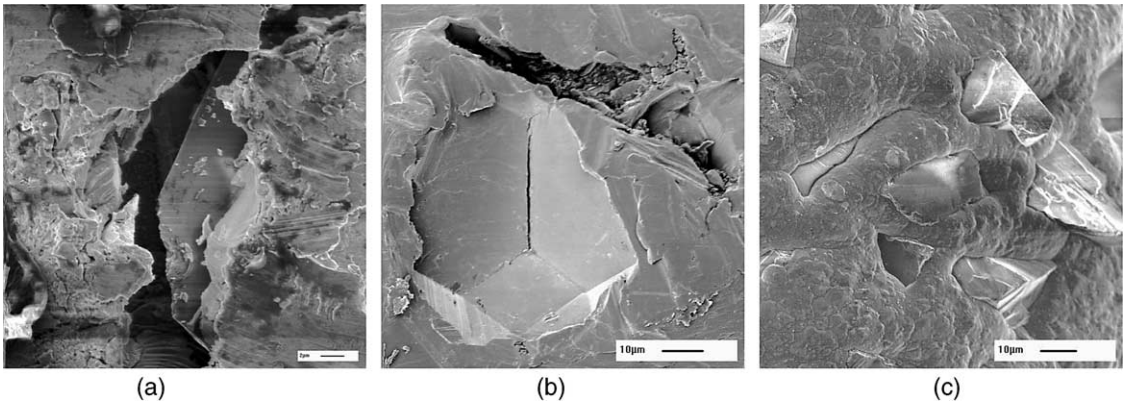

Fig. 4. Close-up view of the diamond grit on new wires. (a) Supplier 1; (b) Supplier 2; (c) Supplier 3.

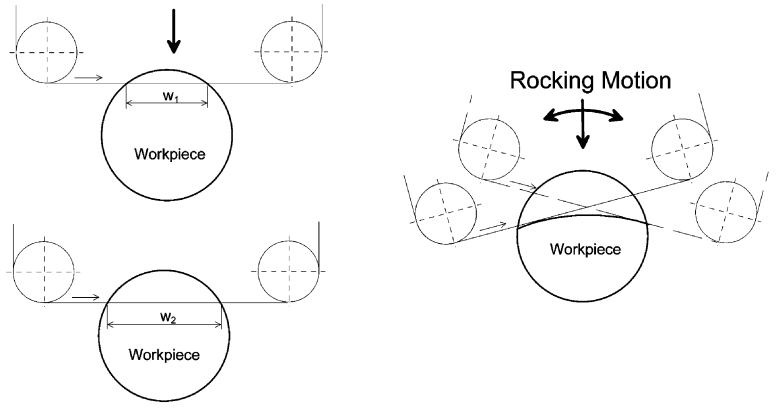

Fig. 5. A comparison of traditional and rocking-motion wire saw machining. (a) Traditional; (b) Rocking motion.

2.3. Rocking motion wire sawing

Fig. 5 illustrates the difference between traditional and rocking motion wire saw machining. The length of contact between the wire and workpiece may change in the traditional wire saw machining, as shown by w_1 and w_2 in Fig. 5(a). The additional rocking motion of either the wire or the workpiece, as shown in Fig. 5(b), can maintain a small and consistent length of contact between the wire and workpiece.

2.4. Non-contact, in-process wire bow sensor

A technology using the capacitance sensor for non-contact, real-time, and in-process measurement of the deflection of the diamond wire during cutting has been developed. The capacitance between the sensor and diamond wire changes as a function of the distance across the face of the sensor. This principle is used to measure the wire deflection without actual contact.

Wire saw machining, including both loose and fixed

abrasive methods, is a relatively new technology. Ito and Murata [1], Tokura et al. [2], and Ishikawa et al. [3] conducted the early wire saw machining experiments. Li et al. [4] presented a model and analysis of the contact between the abrasive and workpiece due to rolling indentation in the free-abrasive wire saw machining of a silicon wafer. Sahoo et al. [5] applied the finite element method to analyze the vibration modes in wire saw cutting of thin wafers. Bhagavat and Kao [6] and Bhagavat et al. [7] presented the finite element analysis of elastohydrodynamic interaction in free-abrasive diamond wire machining.

Most of the breakthroughs in wire saw technology are documented as patents. A survey was conducted on wire saw related patents in the US. A process for cutting brittle semiconductor materials with a diamond wire saw was first developed by Mech [8,9] in the 1970s. There are only three patents in the 1970s [8–10] and two patents in the 1980s [11,12] on the wire saw related machining technology. The number of patents increased slightly before the mid 1990s [13–16] and significantly increased after 1998. Further developments are shown in patents granted in 1998 [17–21], 1999 [22–25], 2000 [26–35], 2001 [36–41] and 2002 [42–46].

This review demonstrates that wire saw machining remains a proprietary technology and there is a lack of research on fixed abrasive diamond wire saw machining. With the needs for continuous improvements in semiconductor, ceramic, and woodworking industries, new diamond wires and wire saw machines are expected to continue evolving to achieve more precise, efficient, and cost-effective machining.

3. Process monitoring in a diamond wire saw

Process monitoring techniques for diamond wire saw machining are investigated using a Millennium diamond wire saw machine, manufactured by Diamond Wire Technology in Colorado Springs, Colorado. This machine, as shown in Fig. 6, utilizes the spool-to-spool model, where a long wire runs between two spools and reverses direction periodically. The motor of the leading wire spool drives the wire to produce the wire movement, and the motor of the trailing wire spool opposes the wire movement to provide the wire tension. The wire speed is selectable between 2.5 and 15 m/s. The wire pre-tension is programmable between 13 and 50 N. Servomotors for spools control the wire tension during cutting. When the wire speed is zero or close to zero during the reversal of direction, two pneumatically preloaded wire tension pulleys are used to maintain the wire tension. Two wire-guide pulleys are moved by a mechanism on the yoke to generate the rocking motion, as shown in Fig. 7. The rocking motion can be set at four frequencies: no rocking, slow (0.15 Hz), medium (0.3 Hz), and fast (0.5 Hz). The angle of wire rock, α, as shown in Fig. 7(d) and (f), is selectable up to 5°.

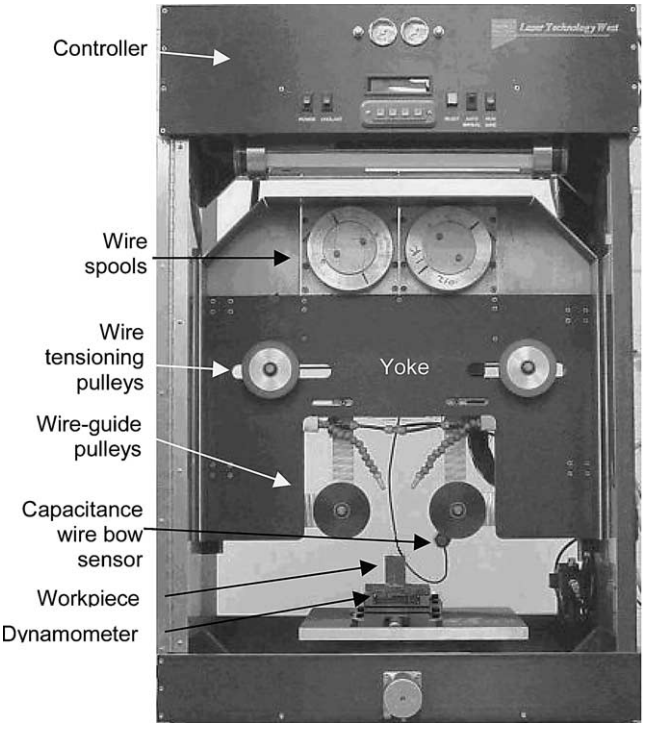

Fig. 6. The spool-to-spool diamond wire saw machine used in this study.

A wire bow sensor, as shown in Fig. 6, is fixed on the rocking mechanism and moved with the wire guide pulleys. The yoke is a slide, which carries wire spools, wire spool motors, wire tension pulleys, wire guide pulleys, and wire guide rocking mechanism. Under the workpiece, a Kistler model 9255B three-axis force dynamometer was used to measure the horizontal and vertical cutting forces, denoted by F_H and F_V.

Five signals are measured by a data acquisition system. Three signals representing the wire bow, yoke position, and wire speed are harnessed from the machine control. Of the three available force channels from the dynamometer, the two channels measuring F_H and F_V are used. The following sections discuss the processing and calibration of these five signals.

3.1. Capacitance sensor for wire bow

During cutting, the diamond wire is subjected to the thrust force that bows the wire. It is necessary to know the amount of wire bow to estimate the cutting force normal to the wire and to know the actual location and orientation of the wire during cutting. A non-contact capacitance sensor, as shown in Fig. 6 and in Fig. 7(a) with diameter D, is used to measure the level wire bow. Major factors that can affect the DC voltage output from the capacitance sensor include: (a) the initial position of

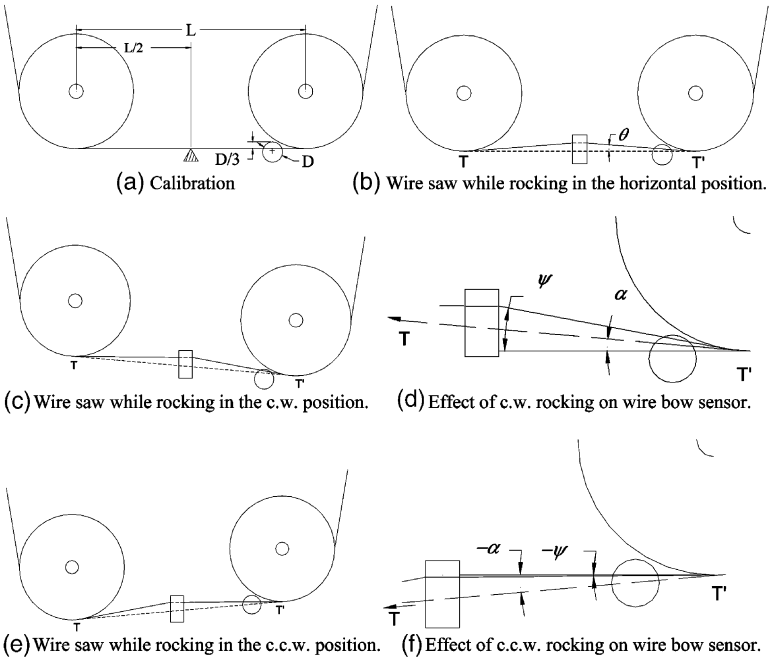

(a) Calibration (b) Wire saw while rocking in the horizontal position.

(c) Wire saw while rocking in the c.w. position. (d) Effect of c.w. rocking on wire bow sensor.

(e) Wire saw while rocking in the c.c.w. position. (f) Effect of c.c.w. rocking on wire bow sensor.

Fig. 7. The setup of capacitance wire bow sensor and the effect of rocking motion on wire bow sensor output.

the horizontal wire in calibration; (b) the distance between two wire guide pulleys; (c) the wire diameter and composition; and (d) the distance between the wire and sensor face. A calibration of the wire bow sensor is necessary before conducting wire saw cutting experiments.

The calibration is conducted using a triangular block to give the point contact at the middle of a pre-tensioned horizontal wire. First, as shown in Fig. 7(a), under a given wire tension, the yoke is moved to guide the wire so that it just touches, but is not deflected by, the tip of the triangular block. At this position, the wire passes across the sensor's face at a height of approximately $D/3$ below the top of the sensor face to accommodate the rocking motion and the wire bow due to vertical cutting force. After inputting the distance L between the guide pulleys' center points, the machine automatically moves the yoke to record the voltage output from 1° to 6° in 1° increments. Fig. 8(a) shows a sample calibration curve of the sensor voltage vs. wire bow angle, θ, shown in Fig. 7(b). During the calibration process, the force dynamometer also measures the vertical force, which is plotted vs. the sensor voltage in Fig. 8(b).

The rocking motion will change the orientation of the wire relative to the bow sensor, which is affixed to the base of the right guide pulley. The orientation of the wire and guide pulleys in the horizontal, clockwise (c.w.), and counterclockwise (c.c.w.) rocking positions is shown in Fig. 7(b), (c), and (e), respectively. The dashed line TT' is tangent to both wire guide pulleys. During wire cutting in the horizontal rocking position, as shown in Fig. 7(b), the wire is deflected by an angle θ. When the pulleys rock by an angle α to the c.w. position, as shown in Fig. 7(d), the angle recorded by the bow sensor is $\psi = \theta + \alpha$. α is positive in the c.w. position and negative in the c.c.w. direction. Note that a small rocking angle is assumed; otherwise, the rotational motion of the capacitance sensor must be factored into the calculation.

Special attention must be taken during cutting in the c.c.w. rocking position. If the absolute value of α is larger than θ, in the c.c.w. position shown in Fig. 7(f), the bow sensor angle ψ is negative and beyond the calibrated region. Fig. 7(f) shows that the wire rocks just past the horizontal to produce a negative angle ψ.

The rocking motion induces a sinusoidal voltage output from the capacitance sensor. An example of the output is shown in Fig. 9(a). The average of peak and trough represents the nominal wire bow angle θ that occurs each time the wire guide pulleys become horizontal to each other. This nominal wire bow angle θ can be used to estimate the vertical cutting force. The piezoelectric dynamometer is not able to measure the vertical cutting force due to the signal decay in tests that last for an extended period of time, more than 8 min in many cases. Using the calibration curve, such as those shown in Fig. 8, the voltage output from the calibrated wire bow sensor can be converted to the nominal wire bow angle θ and vertical cutting force F_V. Fig. 9(b) shows two curves. One is the bow sensor voltage output after localized averaging of the adjacent 32 data points, which present 0.125 s of data under 256 point/s sampling rate. Another is the dark line, obtained from the peak-to-trough averaging of the bow sensor output voltage using the DADISP software. Using the calibration curve in Fig. 8(a), the

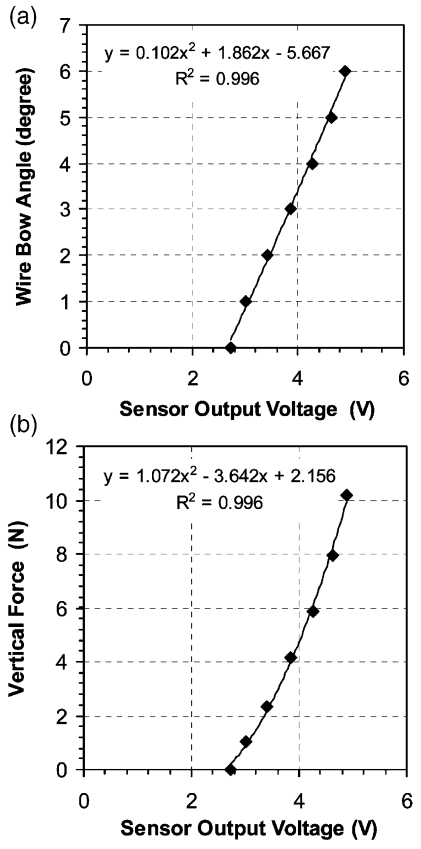

Fig. 8. Sample calibration curves for the capacitance wire bow sensor. (a) Wire bow angle vs. sensor output voltage; (b) Vertical force vs. sensor output voltage.

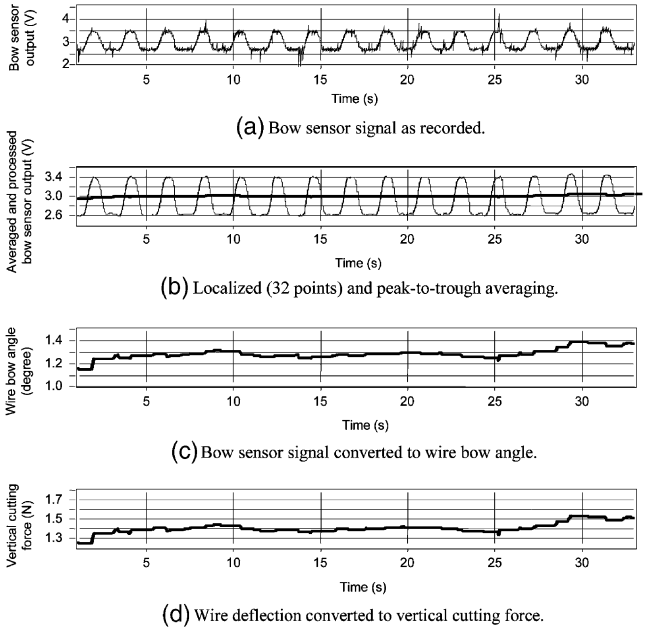

Fig. 9. Capacitance wire bow sensor signal processing.

peak-to-trough averaging line is converted to the wire bow angle θ, as shown in Fig. 9(c). The vertical cutting force, as shown in Fig. 9(d), can be calculated using the calibration curve in Fig. 8(b).

3.2. Yoke stepping motor

A stepping motor controls a ball screw, which drives the yoke up or down to cut into the workpiece. The motor outputs a DC voltage square wave pulse every time it steps. The stepping rate is 250 steps per rotation, and each step moves the yoke by 10.16 μm.

The yoke motor output signal can indicate both the yoke displacement and velocity. By counting the number of pulses and multiplying by the displacement per pulse, the movement of the yoke can be calculated. The frequency of the output pulse from the yoke motor can be multiplied by 10.16 μm/pulse to calculate the yoke speed. An example of the yoke motor voltage output is illustrated in Fig. 10(a). Fig. 10(b) shows the spectrum analysis of the signal in Fig. 10(a). The peak frequency is 5 Hz, which indicates that yoke speed is 0.0508 mm/s.

3.3. Wire speed

The two wire spools that collect and dispense the wire are driven by two servo motors. The leading motor collects the wire and rotates at a set programmed rotational speed. The trailing motor resists the lead motor to provide the wire tension. The diameter of the wire spool determines the wire speed. The base diameter of the wire spool used in this study is 100 mm. As the wire is wrapped on the spool, the diameter of the spool is increased and, therefore, slightly raises the wire speed.

Fig. 11 shows an example of the signal processing for wire speed. The DC voltage of the servomotor angular velocity (tachometer) output is shown in Fig. 11(a). It can be seen that the wire reversal occurs at 3 and 25 s.

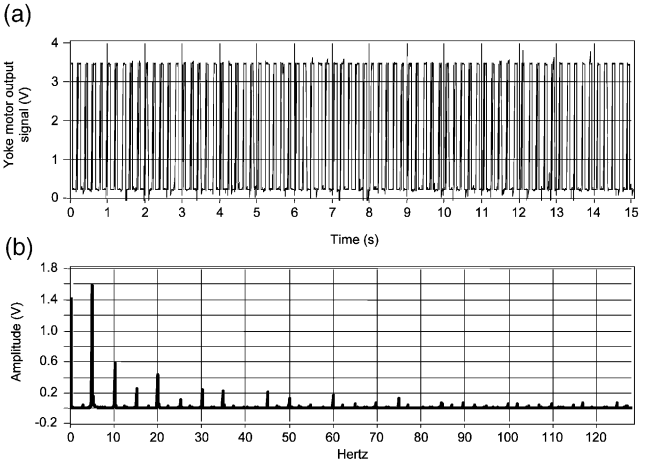

Fig. 10. York motor signal processing. (a) Signal as recorded from the yoke motor; (b) Spectral analysis of the signal.

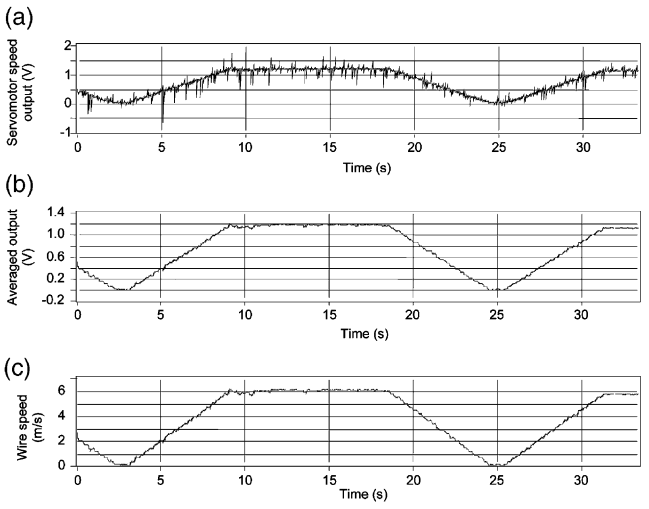

Fig. 11. Wire speed signal processing. (a) Wire speed signal as recorded from servomotor; (b) Localized averaged (32 points) signal; (c) Converted to wire speed.

The gradual increase and decrease in voltage indicates the acceleration and deceleration of wire speed, respectively. The region from 10 to 18 s with constant voltage is the time when the wire has almost constant speed. The servomotor velocity output is averaged to eliminate noise spikes. Results are shown in Fig. 11(b). Based on the 100 mm base diameter of the spool, the angular speed of the spool is converted to wire speed, as shown in Fig. 11(c).

3.4. Horizontal cutting force

As shown in Fig. 6, a Kistler piezoelectric force dynamometer is used to measure the horizontal cutting force. Despite efforts to properly ground the equipment and insulate the data-acquisition device, significant noise was a major problem. Since the noise is random in nature, a high sampling rate and localized averaging was used to minimize it.

Fig. 12 shows the effect of localized averaging on the horizontal force output from the dynamometer. The dynamometer voltage output from the charge amplifier is first converted to the horizontal cutting force and results are shown in Fig. 12(a). Significant noise, which covered the original cutting force data, is observed. The localized average was applied at four levels: 10, 100, 500, and 1000 points. Results are shown in Fig. 12(b)–(e). After locally averaging every 100 points, the trend of changing horizontal cutting force starts to show up. Traces of localized averaging every 500 and 1000 points showed almost identical results. The wire reversed its direction at the 2.5 and 24.5 s and the horizontal cutting force was about 1.5 N.

Using the piezoelectric transducer to measure forces for an extended period of time is ineffective. The charge will gradually decay, which can affect the accuracy of

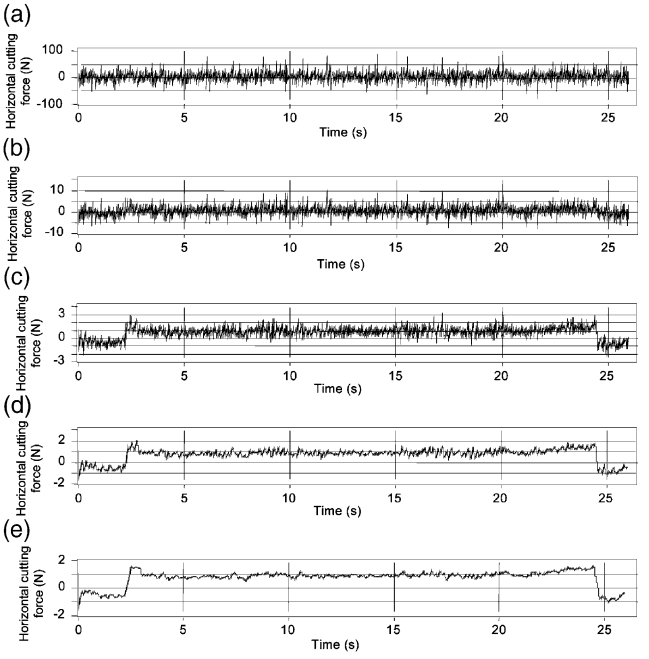

Fig. 12. Effect of localized averaging on horizontal cutting force. (a) Cutting force signal as recorded from dynamometer; (b) Signal after localized averaging of 10 points (0.0024 s); (c) Signal after localized averaging of 100 points (0.024 s); (d) Signal after localized averaging of 500 points (0.122 s); (e) Signal after localized averaging of 1000 points (0.244 s).

the force readings. This decay was observed to have a linear trend. The decay rate was identified and applied to compensate the voltage output data. Fig. 13 shows the three steps to process the data to find the horizontal cutting force. The voltage output from the dynamometer is shown in Fig. 13(a). Using a linear calibration factor for the dynamometer, the voltage output is converted to force, as shown in Fig. 13(b). Localized averaging of every 1000 points is applied (Fig. 13(c)). Lastly, the drift of the dynamometer is corrected to get the horizontal cutting force results shown in Fig. 13(d).

3.5. Vertical cutting force

The piezoelectric dynamometer was unable to measure the vertical cutting force due to the decay and the lack of direction reversals as in the horizontal cutting force. Values of vertical thrust force from the dynamometer remain at about the same level for the duration of a test. Therefore, the capacitance wire bow sensor, as discussed in Section 3.1, was used to estimate the vertical cutting force.

4. Wire tension force during cutting

A model has been developed to analyze the kinematics of rocking motion and the balance of forces in diamond wire cutting.

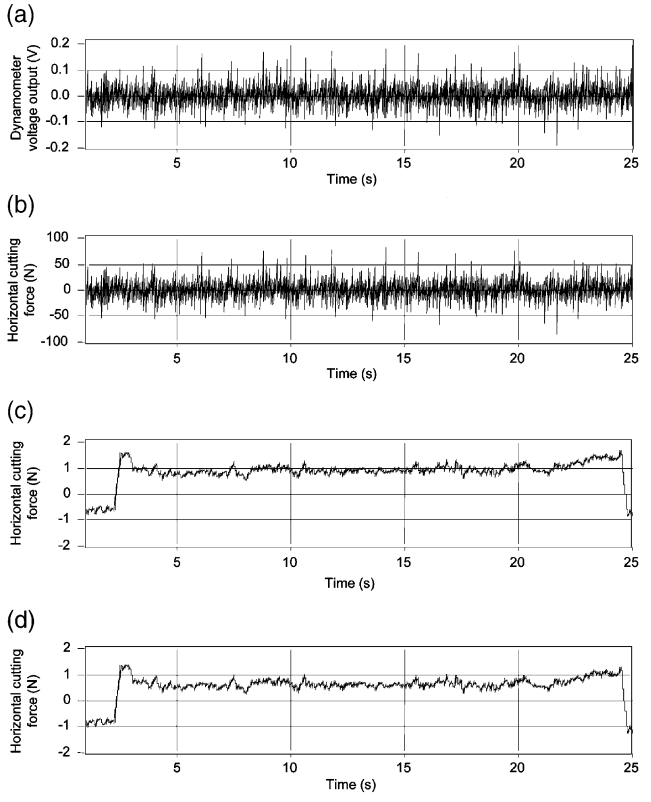

Fig. 13. Cutting force signal processing. (a) Cutting force signal as recorded from dynamometer; (b) Voltage signal converted to vertical cutting force; (c) Signal after localized averaging of 1000 points (0.244 s); (d) Signal corrected for drifting.

4.1. Kinematics of the rocking motion

The mechanism to generate the rocking motion of the yoke in the diamond wire saw machine used in this study is shown in Fig. 14. Two pins in a circular arc slot are used to guide the yoke oscillating around a point, marked by A in Fig. 14, in the middle of the wire between two pulleys. A stepping motor drives a pinion on a circular rack gear to rotate the entire yoke assembly, including wire pulleys, the section of wire between two pulleys, and the capacitance sensor, around point A during cutting.

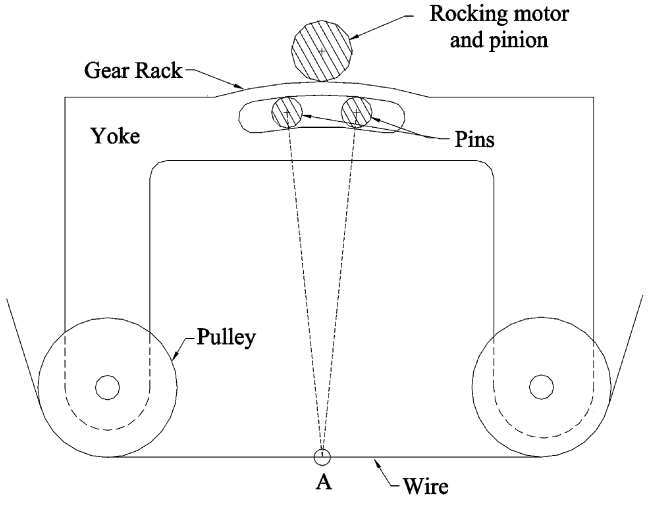

Fig. 14. Kinematics of yoke rocking motion.

4.2. Balance of wire cutting force

Assume the cutting occurs in a narrow area and can be simplified as a point of contact. As shown in Fig. 15, four forces are acting at the point of cutting, marked as B, on the wire. The F_H and F_V are the cutting forces. The wire tension forces are T_1 and T_2 acting in opposite directions. Under the small rocking angle assumption, two wire bow capacitance sensors, as shown in Fig. 15, are used to measure angles ψ_1 and ψ_2, where $\psi_1 = \theta_1 + \alpha$ and $\psi_2 = \theta_2 - \alpha$. θ_1 and θ_2 are the wire bow angles on both sides. The balance of forces at point B can be expressed as:

$$\Sigma F_x = F_H - T_2 \cos \psi_2 + T_1 \cos \psi_1 = 0 \quad (1)$$

$$\Sigma F_y = F_V - T_2 \sin \psi_2 - T_1 \sin \psi_1 = 0 \quad (2)$$

Among the six variables in Eqs. (1) and (2), F_H, F_V, ψ_1, and ψ_2 can be measured. A strain-gauge type dynamometer may be required to measure F_V. Wire tensions T_1 and T_2 can be isolated by rearranging Eqs. (1) and (2).

$$T_1 = \frac{-F_H \sin \psi_2 + F_V \cos \psi_2}{\cos \psi_1 \sin \psi_2 + \cos \psi_2 \sin \psi_1} \quad (3)$$

$$T_2 = \frac{F_H \sin \psi_1 + F_V \cos \psi_1}{\cos \psi_1 \sin \psi_2 + \cos \psi_2 \sin \psi_1} \quad (4)$$

When the cutting point B is in the middle of the wire section between two pulleys, as illustrated in Fig. 7(a) and (b), $\psi_1 = \theta + \alpha$, $\psi_2 = \theta - \alpha$, and only one wire bow sensor is required.

An example using the measured cutting forces and wire bow angles will be presented in the companion paper [47] to show the application of these equations. In actual wire saw cutting, the area of contact is an arc of finite length instead of a point. This remains as a future research topic.

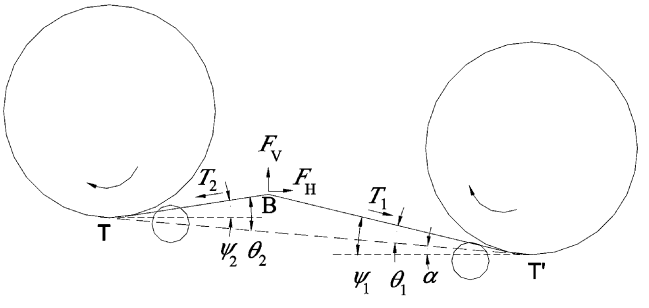

Fig. 15. Force diagram in wire saw cutting.

5. Conclusions

The process monitoring and signal processing methods for fixed abrasive diamond wire machining were developed. A capacitance sensor was applied to measure the wire bow angle in a rocking motion diamond wire saw machine, and the steps to convert the wire bow signal to the vertical cutting force was developed. Localized averaging was found to be important to reduce noise and extract results for the horizontal cutting force. Signal processing of the yoke stepping motor and wire spool servomotor velocity outputs was discussed. The tension force of wire during cutting was explored. This study indicated that more sophisticated process monitoring sensors are required for more complete monitoring of the diamond wire machining process.

Acknowledgements

The authors gratefully acknowledge the Wood Machining and Tooling Research Program (USDA Grant #99-84158-7571) of North Carolina State University and National Science Foundation (Dr K.P. Rajurkar, Program Director). A portion of this research was sponsored by the Assistant Secretary for Energy Efficiency and Renewable Energy, Office of Transportation Technologies, as part of the High Temperature Materials Laboratory User Program, Oak Ridge National Laboratory, managed by UT-Battelle, LLC for the US Department of Energy under contract number DE-AC05-00OR22725.

References

[1] S. Ito, R. Murata, Study on machining characteristics of diamond abrasive wire, Journal of Mechanical Engineering Lab, Tokyo, Japan 41 (5) (1987) 236–244.
[2] H. Tokura, S. Nakayama, M. Yoshikawa, Cutting performance of diamond plated wire tools, Journal of Japan Society of Precision Engineering 58 (12) (1992) 2013–2018.
[3] K. Ishikawa, H. Suwabe, K. Kanayama, M. Makino, H. Yoshida, Study on machining characteristics of wire tool with electrodeposited diamond grains, Transactions of Japan Society of Mechanical Engineers 60 (573) (1994) 1815–1820.
[4] J. Li, I. Kao, V. Prasad, Modeling stresses of contacts in wire saw slicing of polycrystalline and crystalline ingots: application to silicon wafer production, ASME Journal of Electronic Packaging 120 (1998) 123–128.
[5] R.K. Sahoo, V. Prasad, I. Kao, J. Talbott, K.P. Gupta, Towards an integrated approach for analysis and design of wafer slicing by a wire saw, ASME Journal of Electronic Packaging 120 (1998) 35–40.
[6] M. Bhagavat, I. Kao, Computational model for free abrasive machining of brittle silicon using a wiresaw, ASME International Mechanical Engineering Congress and Exposition, Nashville, TN, ASME Design Engineering Division, DE-104, (1999), 21–30.
[7] M. Bhagavat, V. Prasad, I. Kao, Elasto-hydrodynamic interaction in the free abrasive wafer slicing using a wiresaw: modeling and finite element analysis, ASME Journal of Tribology 122 (2) (2000) 394–404.
[8] H. Mech, Machine and method for cutting brittle materials using a reciprocating cutting wire, US patent number, 3,831,576 (1974).
[9] H. Mech, Machine for cutting brittle materials, US patent number, 3,841,297 (1974).
[10] H.B. McLaughlin, Use X and Y table to contour cut the workpiece, US patent number, 4,016,856 (1977).
[11] R.C. Wells, Wire saw, US patent number, 4,494,523 (1985).
[12] R.C. Wells, T.J. Hatfield, Wire saw machine, US patent number, 4,655,191 (1987).
[13] T. Kurokawa, Wire saw, US patent number, 4,903,682 (1990).
[14] N. Takeuchi, Brittle material cutting method, US patent number, 5,201,305 (1991).
[15] K. Toyama, E. Kiuchi, K. Hayakawa, Wire saw and slicing method using the same, US patent number, 5,269,285 (1993).
[16] R. Bonzo, H.G. Shafer, J.P. Trentelman, Apparatus and method for wire cutting glass-ceramic wafers, US patent number, 5,564,409 (1996).
[17] C. Hauser, Wire sawing device, US patent number, 5,758,633 (1998).
[18] C. Hauser, Wire sawing device, US patent number, 5,787,872 (1998).
[19] K. Toyama, Wire saw cutting method synchronizing workpiece feed speed with wire speed, US patent number, 5,810,643 (1998).
[20] C. Hauser, Device for wire sawing provided with a system for directing wire permitting use of spools of wire of very great length, US patent number, 5,829,424 (1998).
[21] J.B. Hodsden, Apparatus and method for slicing a workpiece utilizing a diamond impregnated wire, US patent number, 5,878,737 (1998).
[22] C. Hauser, Wire saw device, US patent number, 5,910,203 (1999).
[23] K. Miyoshi, T. Suzuki, K. Takahashi, Y. Goto, A. Shiba, S. Wada, Wire type slicing machine and method, US patent number, 5,944,007 (1999).
[24] K. Toyama, Wire saw cutting apparatus synchronizing workpiece feed speed with wire speed, US patent number, 5,947,789 (1999).
[25] J.B. Hodsden, Apparatus and method for slicing a workpiece utilizing a diamond impregnated wire, US patent number, 5,964,210 (1999).
[26] J.B. Hodsden, Continuous wire saw loop and method of manufacture thereof, US patent number, 6,065,462 (2000).
[27] S.T. Buljan, R.M. Andrews, Brazed superabrasive wire saw and method therefore, US patent number, 6,102,024 (2000).
[28] K. Egglhuber, Wire saw and method of using it, US patent number, 6,098,610 (2000).
[29] K. Asakawa, H. Oishi, Ingot slicing method and apparatus therefore, US patent number, 6,065,461 (2000).
[30] M. Ikehara, Method using a wire feeding device for a multi-wire saw, US patent number, 6,109,253 (2000).
[31] S. Katamachi, Wire saw for slicing brittle materials with an ingot loading and unloading mechanism, US patent number, 6,135,103 (2000).
[32] I. Ueoka, J. Sugawara, A. Mizogouchi, H. Oshita, M. Yamanaka, H. Ogawa, N. Urakawa, H. Yoshinaga, Wire-saw and its manufacturing method, US Parent Number, 6,070,570 (2000).
[33] D.A. Witte, T. Ragan, Method of slicing silicon wafers for laser marking, US patent number, 6,112,738 (2000).
[34] F.C. Yu, Diamond wire saw, US patent number, 6,105,568 (2000).
[35] J.B. Hodsden, Apparatus and method for slicing a workpiece utilizing a diamond impregnated wire, US patent number, 6,024,080 (2000).
[36] J.B. Hodsden, Rocking apparatus and method for slicing a workpiece utilizing a diamond impregnated wire, US patent number, 6,279,564 (2001).

[37] S. Nagatsuka, S. Okubo, H. Kawarai, H. Oishi, K. Asakawa, J. Matsuzaki, Wire saw control method and wire saw, US patent number, 6,178,961 (2001).
[38] S. Ohashi, M. Matsuzawa, Saw wire assembly, cutting method utilizing the same, and system therefore, US patent number, 6,178,962 (2001).
[39] K. Egglhuber, Wire saw and process for cutting off shaped articles, US patent number, 6,234,159 (2001).
[40] H. Oishi, K. Asakawa, J. Matsuzaki, Wire Sawing Machine, US patent number, 6,237,585 (2001).
[41] K. Onizaki, K. Ogawa, Wire saw cutting method and apparatus therefore, US patent number, 6,283,111 (2001).
[42] O. Kononchuk, G. Preece, Apparatus and method for reducing bow and warp in silicon wafers sliced by a wire saw, magnets using wire saw, and voice coil motor, US patent number, 6,352,071 (2002).
[43] M. Chikuba, H. Ishida, Method for cutting rare earth alloy, method for manufacturing rare earth alloy plates and method for manufacturing rare earth alloy, US patent number, 6,381,830 (2002).
[44] C. Hauser, Wire sawing device for cutting fine slices using angular crossing of at least two sawing yarn layers, US patent number, 6,408,839 (2002).
[45] H. Oishi, K. Asakawa, J., Matsuzaki, K. Ashida, Slurry useful for wire-saw slicing and evaluation of slurry, US patent number, 6,422,067, (2002).
[46] J.B. Hodsden, Continuous wire saw loop and method of manufacture thereof, US patent number, 6,311,684 (2002).
[47] W.I. Clark, A.J. Shih, C.W. Hardin, R.L. Lemaster, S.B. McSpadden, Fixed abrasive diamond wire machining—part II: experiment design and results, International Journal of Machine Tools and Manufacture 43 (2003) 533–542.